International Journal of Mass Spectrometry 283 (2009) 100–104

Contents lists available at ScienceDirect

International Journal of Mass Spectrometry

journal homepage: www.elsevier.com/locate/ijms

SIMION modeling of ion image charge detection in Fourier transform ion cyclotron resonance mass spectrometry

Christopher L. Hendrickson[a,*,1], Steven C. Beu[b], Greg T. Blakney[a], Alan G. Marshall[a,**,1]

[a] Ion Cyclotron Resonance Program, National High Magnetic Field Laboratory, Florida State University, 1800 E. Paul Dirac Drive, Tallahassee, FL 32310-4005, USA
[b] S.C. Beu Consulting, 12449 Los Indios Trail, Austin, TX 78729, USA

ARTICLE INFO

Article history:
Received 30 November 2008
Received in revised form 10 February 2009
Accepted 11 February 2009
Available online 21 February 2009

Keywords:
FT-ICR
FTMS
ICR
Image charge detection
Magnetron

ABSTRACT

We describe a novel SIMION model, based on the principle of reciprocity, to simulate ion–image charge detection and demonstrate utility for Fourier transform ion cyclotron resonance mass spectrometry. The model accommodates arbitrary electrode geometry, magnetic field inhomogeneity, ion-neutral collisions, and swept or single-frequency excitation, but does not account for ion–ion or ion–image charge forces. Accurate frequency-domain spectra reflect actual features of FT-ICR mass spectra including odd and even harmonic multiples of the ion cyclotron frequency, sidebands at odd and even multiples of the trapping frequency, and asymmetric sidebands at even multiples of the magnetron frequency. The model is general and could be applied to other mass analyzers including the quadrupole ion trap, time-of-flight, and orbitrap.

1. Introduction

The development of Fourier transform ion cyclotron resonance (FT-ICR) mass spectrometry [1,2] was enabled by introduction of image charge detection that measures ions by means of the charge induced on nearby electrodes, allowing ion cyclotron motion to be observed for the extended period required to generate high-resolution spectra [3]. The advantages of image charge detection have also been realized in Paul-type ion traps [4–6], time-of-flight instruments [7–10], and most recently the Orbitrap [11]. The continuing evolution of these instruments will benefit from the ability to determine how image charge detection is affected by instrument design and experimental parameters.

Exact solutions for the image charge signal in an ICR cell are generally complex (e.g., multiple infinite sums with terms containing sinusoidal, hyperbolic sinusoidal, and/or Bessel functions), difficult to evaluate (e.g., Green's function methods), and available for only a few highly symmetrical closed electrode structures (e.g., infinitely extended flat parallel plates, cubic, tetragonal (orthorhombic with square cross-section), cylindrical, quadrupolar) [12]. It is therefore more common to approximate the induced charge as proportional to ion displacement in a direction normal to the detection electrodes [3]. Unfortunately, the accuracy of that approach is limited by the unrealistic assumptions that the induced charge is linearly proportional to the radial displacement from the cell (and magnetic field) symmetry (z-) axis and is independent of ion motion along the z-axis.

Here, we apply the principle of reciprocity to accurately simulate three-dimensional image charge within the SIMION [13] modeling environment. We take advantage of SIMION user programs to precisely sample single ion trajectory coordinates in realistic ICR cells and then calculate the potential that exists at each coordinate when appropriate unit potentials are applied to the detection electrodes. Reciprocity dictates that the differential image charge induced by an ion at a given location is proportional to the potential at the same position resulting from application of +1 V and −1 V to the same two opposed electrodes [14,15]. We demonstrate that known nonlinearities in actual FT-ICR spectra can be accurately simulated [16], and discuss the potential of the model to improve FT-ICR cell geometry.

2. Methods

SIMION models were developed to simulate an ICR cell installed in a 9.4 T magnet at the National High Magnetic Field Laboratory [17], which is comprised by three right circular cylinders with equal (9.4 cm) length and diameter (i.e., an open cylindrical ICR cell with aspect (length to width) ratio of two [18]). The potential array resolution was 1 mm per grid unit and each array was

* Corresponding author. Tel.: +1 850 644 0711; fax: +1 850 644 1366.
** Corresponding author. Tel.: +1 850 644 0529; fax: +1 850 644 1366.
E-mail addresses: hendrick@magnet.fsu.edu (C.L. Hendrickson), marshall@magnet.fsu.edu (A.G. Marshall).
[1] Also a member of the Department of Chemistry and Biochemistry, Florida State University, Tallahassee, FL 32306, USA.

1387-3806/$ – see front matter © 2009 Elsevier B.V. All rights reserved.
doi:10.1016/j.ijms.2009.02.009

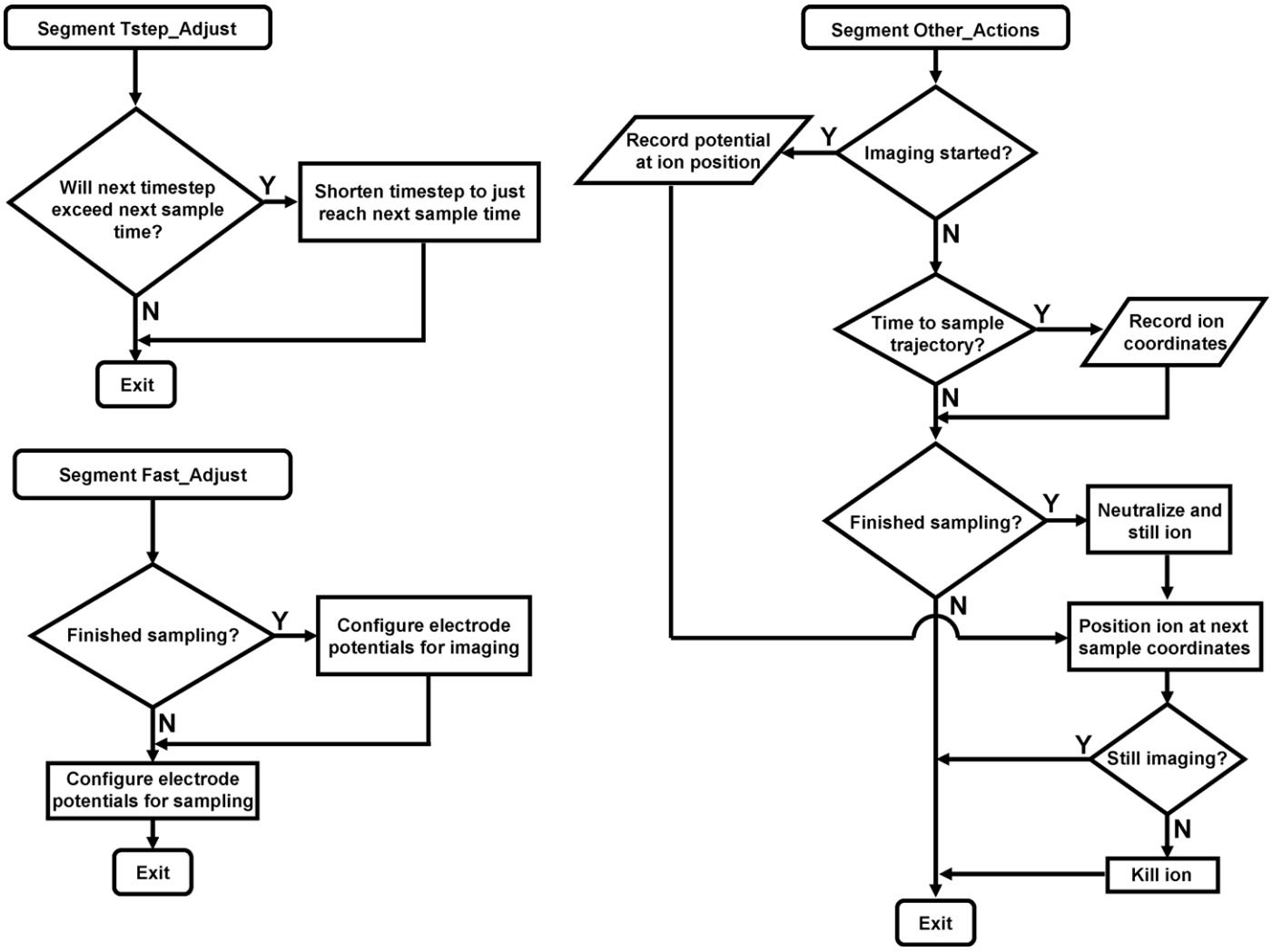

Fig. 1. Flow charts for SIMION user program components for implementation of ion image charge modeling.

refined to a precision of 10^{-6}. A SIMION user program was developed to implement reciprocity-based image charge determination (Fig. 1) as follows. Ion trajectories are first acquired with user specified FT-ICR MS parameters and concurrently sampled at a specified rate (typically 5 MHz for 52 ms). The model allows specification of trap potentials (typically 1 V in this work), excitation mode (i.e., single-frequency or frequency-sweep) and potential (alternatively, ion cyclotron radius can be specified), ion-neutral collision [19] parameters, and solenoidal magnetic field inhomogeneity [20] (we neglected collisions and magnetic field inhomogeneity in the simulations reported here). The dynamic time-step adjustment algorithm employed by the SIMION trajectory calculation was modified to allow sampling of the trajectory coordinates at precise, equal temporal intervals, as required for subsequent Fourier transform. After sampling is concluded, the cell electrode potentials are reset to the reciprocity values and the ion charge and velocity components set to zero to avoid any subsequent field-induced movement. The neutralized ion is then sequentially relocated to each of the sampled trajectory coordinates and the potential at that point recorded. In accordance with the principle of reciprocity, the differential image charge induced between a pair of detection electrodes by a unit charge located at each trajectory point was obtained from the potential that exists at that point when opposite-sign unit potentials are applied to the detection electrodes and all other cell electrodes are grounded [12,14,15,21,22]. Ion mass and charge, as well as ion initial position, kinetic energy, and cyclotron radius can be specified and incremented for each ion modeled in batch mode. The sampled trajectory coordinates and corresponding image charge values for all modeled ions were stored in a single text file and subsequently converted into individual ion image signal transients based on a primarily capacitive detection circuit model [3]. Time-domain transients were converted to frequency-domain spectra by conventional means (e.g., apodization, one zero-fill, FFT, and magnitude calculation [23]) with MIDAS analysis processing software [24]. All simulations were performed with SIMION 3D (Version 7, Idaho National Engineering and Environmental Laboratory, Idaho Falls, ID) running on either a homebuilt AMD 64 X2 5600+dual processor with 2 GB ram or a 2.6 GHz Pentium Core 2 Duo laptop with 2 GB ram (Latitude 830, Dell Inc., Austin, TX).

3. Results and discussion

FT-ICR spectra derived from reciprocity-based simulation of ion image current are strikingly similar to experimental data collected from our 9.4 T FT-ICR mass spectrometer [17] and exhibit nonlinearities that are absent or inaccurately represented by prior methods based on radial coordinate analysis. Examples include signals at harmonics of the ion cyclotron frequency, resulting from truncated electrodes and/or uncentered ion cyclotron motion, as well as modulation sidebands resulting from ion axial oscillation and magnetron rotation.

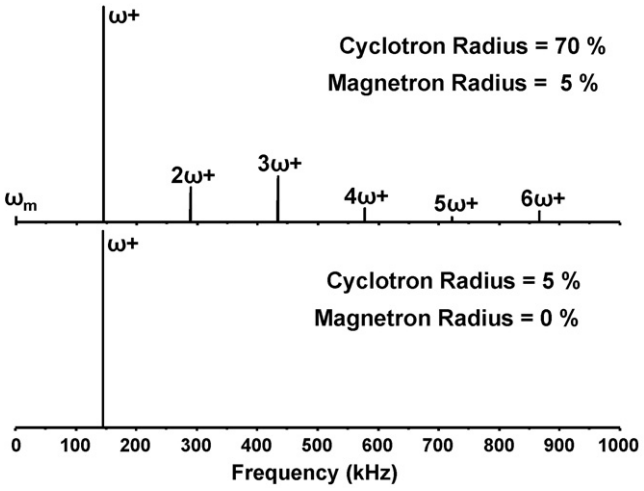

Fig. 2. Frequency-domain FT-ICR spectrum of an m/z 1000 ion modeled by ion image charge analysis for cyclotron orbital radius of 70% and magnetron orbital radius of 5% of the cell radius (top) and for cyclotron orbital radius of 5% and magnetron orbital radius of 0% of the cell radius (bottom). Note the prominence of analytically predicted odd (at high cyclotron radius) and even (at non-zero magnetron radius) harmonics of the cyclotron frequency in the top spectrum.

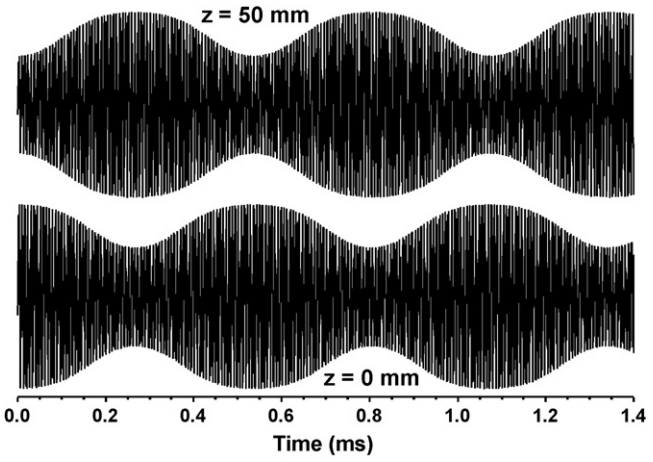

Fig. 3. Ion image charge versus time modeled for an m/z 1000 ion with initial axial (z-) displacement from the ICR cell center of z = 50 mm (top) and z = 0 mm (bottom), when ion axial amplitude is 50% of the axial potential well length and the cyclotron orbital radius is 50% of the cell radius. Note the analytically predicted amplitude modulation.

3.1. ICR harmonics

Signals at odd harmonics of the fundamental ion cyclotron frequency are predicted analytically [12,25] and observed experimentally for all real ICR cell geometries (and can potentially be utilized to increase mass resolving power [22,26–30]). SIMION image charge modeling exhibits odd harmonics, whereas modeling based on ion radial coordinates does not. Further, if the cyclotron orbit is displaced radially (i.e., non-zero magnetron radius, as typically results from ion injection from an external source and/or from frequency-sweep excitation [31]) image charge modeling predicts both odd and even harmonic signals (Fig. 2). The magnitude for each harmonic depends critically on the cell geometry (as well as the ion motional amplitudes) [26–27]; thus, a given cell configuration can be quickly evaluated for sensitivity and linearity. For example, we have shown that increase in azimuthal extent of the detection electrodes improves sensitivity (by as much as 41%) in square and circular cross-section ICR cells, but requires an equivalent decrease in excitation electrode angular extent. Further, the magnitude of specific harmonic peaks can be reduced or even eliminated by appropriate choice of detection electrode angular extent [32].

3.2. Trapping sidebands

Ion axial oscillation during detection may generate signals displaced equally above and below the cyclotron frequency by the axial oscillation ("trapping") frequency, due to the periodic amplitude modulation shown in Fig. 3. Analytical treatments predict that the sidebands should be displaced by even multiples of the axial oscillation frequency away from the cyclotron peak [12]. Here again, image charge modeling reveals the effect (Fig. 4 top), whereas radial coordinate analysis does not.

Nevertheless, most experimental FT-ICR spectra do not exhibit significant trapping sidebands because the detected signal results from incoherent summation of signals from ions of significantly different axial oscillation phase, due to the typically substantial distribution in arrival time (and thus initial ion axial position at the onset of detection) for ions of a given m/z. For example, Fig. 4 (bottom) shows the sum of two simulated transients that differ in initial phase by 90°, resulting in nearly complete cancellation of the largest sidebands (the small sidebands spaced at 4 times the trapping frequency (due to the second harmonic content of the modulation frequency) are eliminated by sum of two transients that differ by 45°). In general, summation of many ion signals with incoherent initial axial phase will reduce the relative magnitude of the sidebands by $n^{1/2}$ (where n is the number of signals; the in-phase ICR signal magnitude increases linearly with n, whereas the incoherent sideband amplitudes increase with $n^{1/2}$), just as summation of many ICR transients increases the signal-to-noise ratio by the same factor [23].

Detection of sidebands displaced by odd harmonics of the axial frequency has also been reported [33], and attributed to misalignment between the ICR trap and the magnetic field symmetry (z-) axis [12]. Image charge modeling reveals that even a 3° misalignment does not result in observable odd-harmonic sidebands (Fig. 5, top). However, odd-harmonic sidebands are observed if the center of the ion axial oscillation is offset from the axial center of the detection electrodes (Fig. 5, bottom), as could arise from application of high voltage to electrodes near the ICR cell (particularly for an open

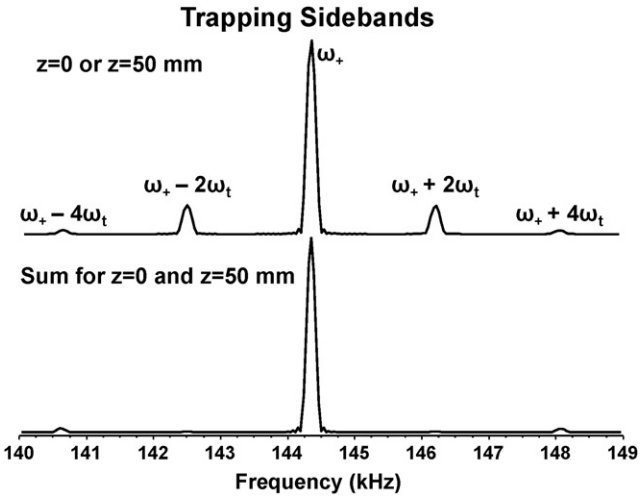

Fig. 4. Frequency-domain FT-ICR spectra derived by Fourier transform of: (top) either the 0° or 90° phase ion signal shown in Fig. 3 and (bottom) the Fourier transform of the sum of the 0° and 90° phase ion signals shown in Fig. 3. Note that the trapping sidebands are diminished by destructive interference on summation of ion signals of varying phase.

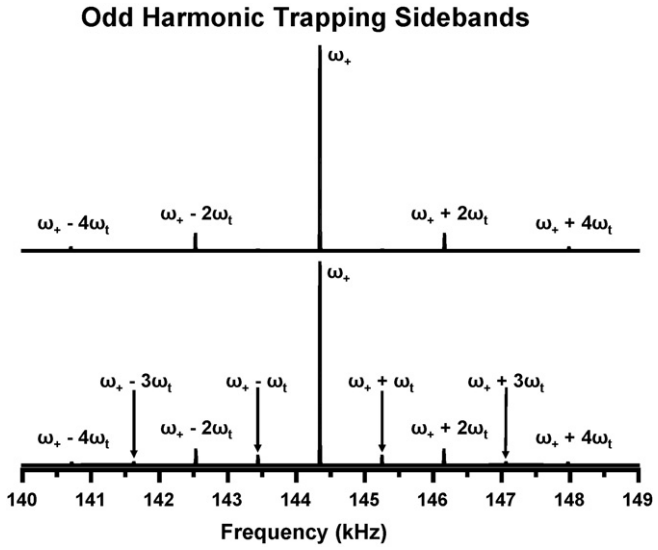

Fig. 5. Frequency-domain FT-ICR spectra of an m/z 1000 ion derived from image charge determination when the trap axis and magnetic field are misaligned by 3° (top) or the center of axial oscillation is displaced axially by 5 mm (bottom). Only the bottom spectrum exhibits sidebands at odd multiples of the trapping frequency.

cell). As with the even harmonics discussed above, the odd harmonics are not expected to be observed in a large population of ions with varying initial axial phase, but the magnitude of the observed cyclotron signal is reduced by amplitude modulation, which can be easily quantified by our model.

3.3. Magnetron sidebands

Ion magnetron motion can also modulate the ICR signal amplitude, resulting in sidebands displaced above and below the cyclotron frequency. Theory predicts sidebands spaced at even harmonics of the magnetron frequency [34], as confirmed by image charge modeling. Further, the model predicts significant asymmetry of sideband amplitude analogous to Mitchell's prediction for nonlinear ion excitation resonance in a cubic ICR trap [35,36]. As shown in Fig. 6, only the higher frequency sideband is evident when significant magnetron displacement is modeled (magnetron radius = 10% of the cell radius in Fig. 6). The magnetron frequency scales linearly with trap potential and inversely with magnetic field, so that at high magnetic field and low trap potential, that sideband may not be resolved from the cyclotron peak and may therefore be interpreted as peak splitting or "tailing" [37].

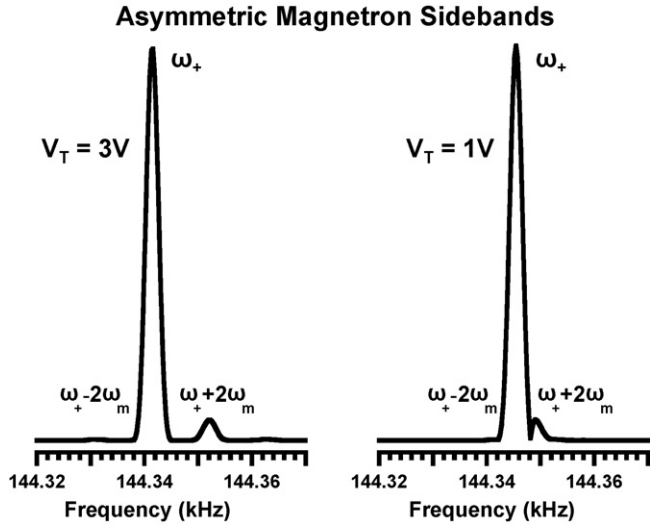

Fig. 6. Frequency-domain FT-ICR spectra of an m/z 1000 ion derived by image charge determination for magnetron radius equal to 1 cm and trap potential equal to 3 V (left) and 1 V (right). Note magnetron sidebands with unequal amplitudes.

4. Conclusion

A reciprocity-based SIMION model accurately represents ion image charge during ion trajectory analysis. Application to a commonly used open cylindrical FT-ICR cell configuration yields FT-ICR frequency-domain spectra that exhibit many experimentally familiar nonlinearities, including harmonic multiples of the fundamental cyclotron frequency and sidebands displaced equally above and below the cyclotron frequency by multiples of the axial oscillation ("trapping") frequency and magnetron frequency. In addition the model can accommodate arbitrary electrode configuration, magnetic field inhomogeneity, ion-neutral collisions, and swept frequency ion excitation. Careful quantitative analysis of spectral nonlinearities and sensitivity offers great promise for design of more sensitive and linear ICR cell configurations, as well as those for other mass analyzers.

Acknowledgments

This work is dedicated to Professor Michael T. Bowers on the occasion of his 70th birthday and was supported by the NSF National High-Field FT-ICR Mass Spectrometry Facility (DMR-06-54118), Florida State University, and the National High Magnetic Field Laboratory at Tallahassee, FL.

References

[1] M.B. Comisarow, A.G. Marshall, Chem. Phys. Lett. 25 (1974) 282.
[2] A.G. Marshall, C.L. Hendrickson, G.S. Jackson, Mass Spectrom. Rev. 17 (1998) 1.
[3] M.B. Comisarow, J. Chem. Phys. 69 (1978) 4097.
[4] R.G. Cooks, C.D. Cleven, L.A. Horn, M. Nappi, C. Well, M.H. Soni, R.K. Julian, Int. J. Mass Spectrom. Ion Processes 146–147 (1995) 147.
[5] M.W. Senko, J.C. Schwartz, A.E. Schoen, J.E.P. Syka, in: Fouier Transform Mass Spectrometry in a Linear Quadrupole Ion Trap, Proc. 48th Amer. Soc. Mass Spectrom. Conf. on Mass Spectrom. & Allied Topics, Long Beach, CA, Am. Soc. Mass Spectrom. (2000), p TOE pm 03:00.
[6] J.E.P. Syka, W.J. Fies Jr., Fourier transform quadrupole mass spectrometer and method, US Patent 4,755,670 (1988).
[7] W.H. Benner, Anal. Chem. 69 (1997) 4162.
[8] G. Hars, I. Maros, Int. J. Mass Spectrom. 225 (2003) 101.
[9] M. Park, J.H. Callahan, Inductive detector for time-of-flight mass spectrometers, US Patent 5,591,969 (1997).
[10] M.A. Park, J.H. Callahan, Rapid Commun. Mass Spectrom. 8 (4) (1994) 317.
[11] A. Makarov, Anal. Chem. 72 (2000) 1156.
[12] P.B. Grosshans, P.J. Shields, A.G. Marshall, J. Chem. Phys. 94 (1991) 5341.
[13] D.A. Dahl, Int. J. Mass Spectrom. 200 (2000) 3.
[14] R.C. Dunbar, Int. J. Mass Spectrom. Ion Processes 56 (1984) 1.
[15] W. Shockley, J. Appl. Phys. 9 (1938) 635.
[16] S.C. Beu, C.L. Hendrickson, A.G. Marshall, in: SIMION Modeling of Image Charge Detection in FT-ICR MS, Proc. 54th Amer. Soc. Mass Spectrom. Conf. on Mass Spectrom. & Allied Topics, Seattle, WA, Am. Soc. Mass Spectrom. (2006), p MP10 212.
[17] K. Håkansson, M.J. Chalmers, J.P. Quinn, M.A. McFarland, C.L. Hendrickson, A.G. Marshall, Anal. Chem. 75 (13) (2003) 3256.
[18] S.C. Beu, D.A. Laude Jr., Int. J. Mass Spectrom. Ion Processes 112 (1992) 215.
[19] A.D. Appelhans, D.A. Dahl, Int. J. Mass Spectrom. 216 (3) (2002) 269.
[20] D.W. Mitchell, A.L. Rockwood, R.D. Smith, Int. J. Mass Spectrom. Ion Processes 141 (2) (1995) 101.
[21] D.L. Rempel, S.K. Huang, M.L. Gross, Int. J. Mass Spectrom. Ion Processes 70 (1986) 163.
[22] A.S. Misharin, R.A. Zubarev, Rapid Commun. Mass Spectrom. 20 (2006) 3223.
[23] A.G. Marshall, F.R. Verdun, Fourier Transforms in NMR, Optical, and Mass Spectrometry: A User's Handbook, Elsevier, Amsterdam, 1990, p. 460.
[24] G.T. Blakney, G. van der Rest, J.R. Johnson, D.M. Horn, M.A. Freitas, J.J. Drader, S.D.-H. Shi, C.L. Hendrickson, N.L. Kelleher, A.G. Marshall, in: Further Improvements to MIDAS Data Station for FT-ICR Mass Spectrometry, Proc. 49th Amer. Soc. Mass Spectrom. and Allied Topics, Chicago, IL, Am. Soc. Mass Spectrom. (2001), p WPM 265.
[25] E.N. Nikolaev, M.V. Gorshkov, Int. J. Mass Spectrom. Ion Processes 64 (1985) 115.

[26] P.B. Grosshans, A.G. Marshall, Int. J. Mass Spectrom. Ion Processes 107 (1991) 49.
[27] M. Knobeler, K.P. Wanczek, Int. J. Mass Spectrom. Ion Processes 125 (1993) 127.
[28] P.A. Limbach, P.B. Grosshans, A.G. Marshall, Int. J. Mass Spectrom. Ion Processes 123 (1993) 41.
[29] E.N. Nikolaev, M.V. Gorshkov, A.V. Mordehai, V.L. Talrose, Rapid Commun. Mass Spectrom. 4 (1990) 144.
[30] Y.P. Pan, D.P. Ridge, A.L. Rockwood, Int. J. Mass Spectrom. Ion Processes 84 (1988) 293.
[31] M. Wang, A.G. Marshall, Int. J. Mass Spectrom. Ion Processes 100 (1990) 323.
[32] C.L. Hendrickson, S.C. Beu, A.G. Marshall, in: Optimized Image Current Detection Geometry for Fourier Transform Ion Cyclotron Resonance Mass Spectrometry, Proc. 56th Amer. Soc. Mass Spectrom. Conf. on Mass Spectrom. & Allied Topics, Denver, CO, Am. Soc. Mass Spectrom. (2008), p MOC pm 02:30.
[33] D. Mitchell, S. Delong, D. Cherniak, M. Harrison, Int. J. Mass Spectrom. Ion Processes 91 (1989) 273.
[34] A.G. Marshall, P.B. Grosshans, Anal. Chem. 63 (1991) 215A.
[35] D.W. Mitchell, B.A. Hearn, S.E. DeLong, Int. J. Mass Spectrom. Ion Processes 125 (1993) 95.
[36] S.K. Shin, S.-J. Han, Int. J. Mass Spectrom. 153 (1996) 87.
[37] S.C. Beu, G.T. Blakney, J.P. Quinn, C.L. Hendrickson, A.G. Marshall, Anal. Chem. 76 (2004) 5756.